Supporting Information

Fast Ionic Transport in $SrTiO_3/LaAlO_3$ Heterostructure

Quan Shi, [a#] Haijian Zhong, [b#] Ming Huang, [c] Bin Zhu[a], Liwen Huang, [a] Yan Wu[*a]

[a]Engineering Research Center of Nano-Geo Materials of Ministry of Education, Faculty of Materials Science and Chemistry, China University of Geosciences, 388 Lumo Road, Wuhan 430074, China

[b]School of Medical and Information Engineering, Gannan Medical University, Ganzhou 341000, China

[c]Faculty of Physics and Electronic Sciences, Hubei University, Wuhan 430062, China

[#]These authors contributed equally.

Corresponding authors: wuyan@cug.edu.cn (Y. Wu)

Experimental procedures

Materials synthesis

All the chemical agents were purchased from Sinopharm chemical reagent co. LTD, including $Sr(NO_3)_2$, $Ti(C_4H_9O)_4$, ethylene glycol (EG), NaOH, citric acid, $La(NO_3)_3$ and $Al(NO_3)_3 \cdot 9H_2O$ in analytical grade.

$SrTiO_3$ was synthesized by sol-gel hydrothermal method.[1] 0.01 mol $Sr(NO_3)_2$ was dissolved in 20 ml EG solvent with continuous stirring at 80 ^oC until the solution was completely transparent. Subsequently, 0.01 mol $Ti(C_4H_9O)_4$ was gradually added to the above solution to form a sol gradually. Then a NaOH solution (5 mol/L) was dropped into the sol to form the gel with stirring and aged for 30 min at 80 ^oC. Then the gel was poured into a 100 ml stainless reaction kettle and kept for 24 h at 200 ^oC, cooling down to room temperature. The obtained sediment was washed with distilled water until the pH value was close to 7 and dried at 80 ^oC.

The $LaAlO_3$ powder was synthesized by sol-gel method.[2] The molar ratios of EG, citric acid, $La(NO_3)_3$ and $Al(NO_3)_3 \cdot 9H_2O$ were 20:10:1:1. Firstly, the required amounts of EG and citric acid were dissolved in deionized water. The appropriate amounts of $La(NO_3)_3$ and $Al(NO_3)_3 \cdot 9H_2O$ were added to the solution. Then, the solution was heated up to 80 ^oC, accompanied with vigorous stirring for 3 h until the gel formed. The gel was calcinated in the oven at 200 ^oC over 6 h for removing the moisture, and then the gel turned yellow from white color. Subsequently, the yellow gel was put in a muffle furnace at 300 ^oC (at a heating rate of 10 $^oC \cdot min^{-1}$) for 2 h to obtain the precursor. Then the precursor was grounded and calcined at 900 ^oC (at a heating rate of (10 $^oC \cdot min^{-1}$) for 6 h to get the LAO powders.

The STO/LAO composites were synthesized by a similar sol-gel method based on the synthesized $SrTiO_3$ nanoparticles. The necessary amounts of STO powder were added into the first step of the solution in the synthesis of $LaAlO_3$with EG, citric acid, $La(NO_3)_3$, $Al(NO_3)_3 \cdot 9H_2O$ and distilled water. The rest of the steps was the same as that of the $LaAlO_3$ preparation. Finally, the composites with different constitutions of 0.4STO/0.6LAO, 0.5STO/0.5LAO, 0.6STO/0.4LAO and 0.7STO/0.3LAO were obtained.

Fuel cell construction

The fuel cells were fabricated in a configuration of Ni-NCAL ($Ni_{0.8}Co_{0.15}Al_{0.05}$Li-oxide)

/STO/LAO/ NCAL-Ni, in which the STO/LAO composites were sandwiched between two Ni-NCAL round pieces. The cell was assembled by one step pressing under a load of 200 MPa to form a pellet with 1.5 mm in thickness and 13 mm in diameter with an active area of 0.64 cm^2. The NCAL was purchased from Tianjin Bamo Sci. & Tech. Joint Stock Ltd., China. The NCAL was coated in a porous Ni piece with 2 mm thickness to form an electrode on both sides of the STO/LAO membrane as the fuel cell device. Subsequently, the device was heated to 520 ^oC and kept for 30 minutes before fuel cell measurements. After keeping cell for 30 minutes at 520 ^oC, the hydrogen and ambient air were supplied to anode and cathode at atmospheric pressure as fuel and oxidant, respectively. The flow rate of the air and H_2 were set at 120- and 90-ml min^{-1}, respectively.

Materials characterization

The crystal structures of as-prepared samples were investigated by using an X-ray diffractometer (XRD, D8FOCUS Bruker Germany) with Cu Kα radiation (λ=1.54060 Å) as the source. A field emission scanning electron microscope (FE-SEM, Merlin Japan) equipped with EDS (Energy dispersive spectrometer) was used for analyzing the microstructure and the component of the samples. X-ray photoelectron spectrum (XPS, Thermo Scientific K-Alpha 250XI) was carried out at room temperature with a source gun type of Al K Alpha. The instrument was operated in a standard lens mode and computer analyzer mode with an energy step size of 0.050 eV. The C 1s (284.6 eV) was selected as an internal standard to calibrate binding energy. High-resolution transmission electron microscopy (HRTEM) images were acquired by using the Tecnai G2 F30 operated at an acceleration of 200 kV. In addition, all the samples for HRTEM test were first supersonic dispersed in ethanol for a half hour and then dipped onto 400 mesh Cu grid, followed by drying in air. The atomic force microscopy (AFM) image was obtained by using the Multi Mode 8 (Bruker, USA) at tapping mode. The 0.3 g sample was pressed at 350 MPa for 5 minutes to form the pellet with the flat surface.

The electrochemical impedance spectra (EIS) were carried out by using a chemical workstation (Zennium E, Zahner, Germany) between 520 ^oC and 430 ^oC. The applied frequency ranged from 0.1 MHz to 0.1 Hz with an amplitude of 0.01 Hz. The digital instrument (ITECH8511, ITECH Electrical Co., LTD.) was used for measuring cell voltage, power density, and current density to

draw *I-V* (current-voltage) and *I-P*(current-power) characteristics.

DFT calculations.

The density-functional theory (DFT) calculations were performed with generalized gradient approximation (GGA) by Perdew-Burke-Ernzerhof (PBE) functional and all-electron projector augmented wave (PAW) method as implemented in Vienna ab initio simulation package (VASP) code.[3-6] An energy cutoff of 500 eV for the plane-wave basis set was adopted. The k-points grids of 9×9×1 using Γ-center schemes were used to sample the first Brillouin zone. All the geometry structures are fully relaxed until the total energy converged to 1.0×10^{-5} eV and the forces on each atom were smaller than 0.02 eV/Å. To get accurate electronic, the electronic structures of STO/LAO heterostructure and the density of states are computed based on the HSE06 functional.[7]

Table S1- Equivalent circuit analysis results of all samples at 520 °C.

Sample (550 °C)	R_b (Ω cm^2)	R_{gb} (Ω cm^2)	R_{ct} (Ω cm^2)
0.4STO/0.6LAO	0.577	0.261	0.155
0.5STO/0.5LAO	0.415	0.184	0.188
0.6STO/0.4LAO	0.519	0.382	0.210

Table S2- The peak position of different oxygen species. During the peak fitting, the Lorentzian/Gaussian ratio of all elements was fixed to 0.3, in additional the full width at half maximum (FWHM) of spin couplet peak of one element in the same chemical state was kept as a value. Area1 and Area2 represent the area of Peak O_L and Peak O_C, respectively.

`	O_L (eV)	O_C (eV)	Area1 (eV)	Area2 (eV)	Area2/(Area1+Area2)
LAO	528.76	531.17	108760	26304	0.19
STO	529.12	531.00	131595	38137	0.22
0.5STO/0.5LAO	528.68(LAO) 529.24(STO)	531.00	60153(LAO) 47171(STO)	35947	0.25
50.5STO/0.5LAO (After cell operation)	528.70(LAO) 529.35(STO)	531.41	81169(LAO) 61792(STO)	52450	0.27

Supplementary Note 1

The conductivity is calculated according to the equation (1):

$$\sigma = \frac{L}{SR} \qquad (1)$$

where L represents the length, and S is the area, and the total resistance (R) is obtained by EIS.

The activation energy of the STO/LAO composites can be calculated by plotting ln(σT) versus 1000/T according to the Arrhenius equation (2):

$$\sigma T = Aexp^{(\frac{-Ea}{KT})} \qquad (2)$$

Here, A is a pre-exponential factor, T is the absolute temperature, E_a is the activation energy, and K is the Boltzmann constant.

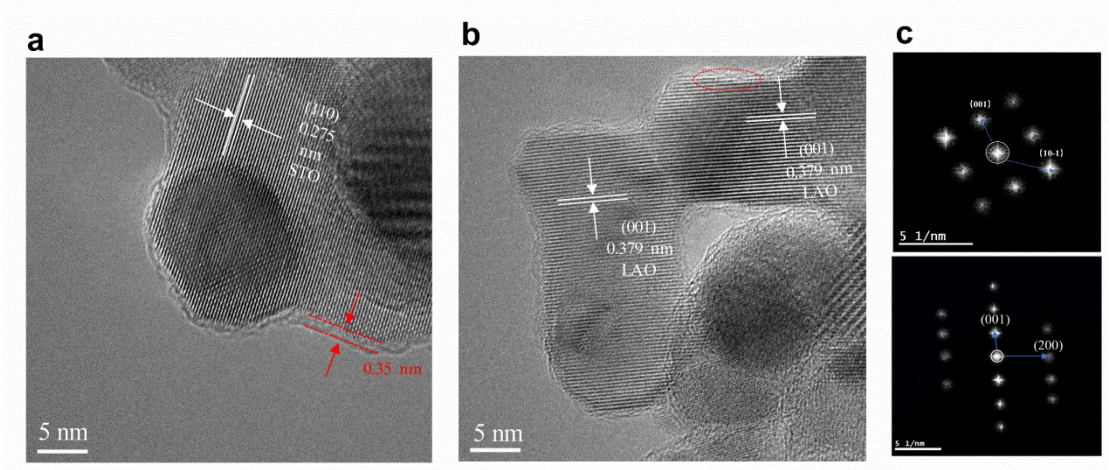

Figure S1. Transmission electron micrograph of STO and LAO crystals. (a) High-resolution transmission electron micrograph (HRTEM) image of STO particle, and (b) HRTEM image of LAO particle, and top graph of (c) the selected area electron diffraction (SAED) pattern of STO particle, and below graph of (c) the SAED pattern of LAO particle. The area marked by red dotted line and circle in (a) and (b) represent the amorphous layer.

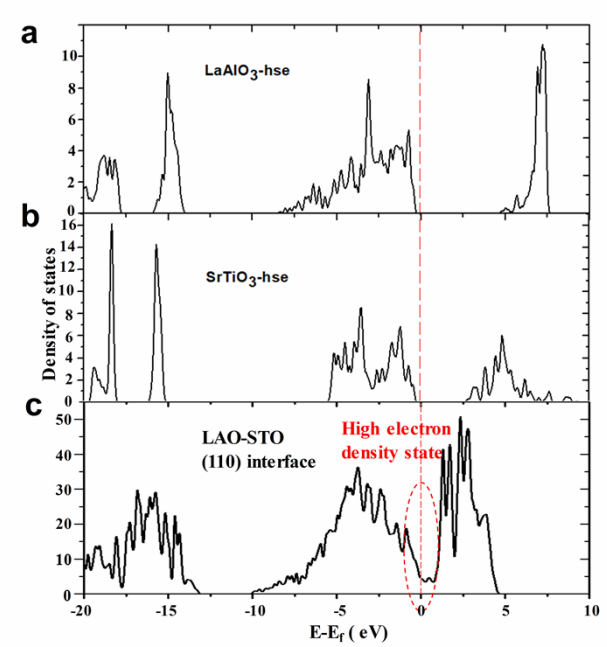

Figure S2. DFT calculation results of STO (a), LAO (b), and STO/LAO (110) interface (c).

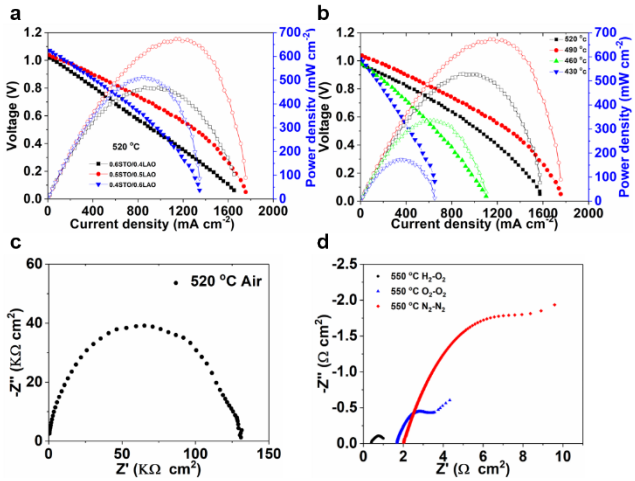

Figure S3. The application of STO/LAO hetero-composite at SCFC. (a) *I-V* and *I-P* curve of fuel cell based on STO/LAO composites, and (b) *I-V* and *I-P* curve of fuel cell based on 0.5STO/0.5LAO composite. (d) Impedance spectra of 0.5STO/0.5LAO cells in air condition on 520 °C. (d) EIS result of the cell based on 0.5STO/0.5LAO under H_2/O_2, O_2/O_2, N_2/N_2 atmosphere.

References:

1. Yu, H., Yan, S., Li, Z., Yu, T., Zou, Z. (2012). Efficient visible-light-driven photocatalytic H_2 production over Cr/N-codoped $SrTiO_3$. International Journal of Hydrogen Energy. 37, 12120–12127.
2. Silva, C.A.D., Miranda, P.E.V.D. (2015). Synthesis of $LaAlO_3$ based materials for potential use as methane-fueled solid oxide fuel cell anodes. International Journal of Hydrogen Energy. 40, 10002–10015.
3. Perdew, J.P., Burke, K., Ernzerhof, M. (1996). Generalized gradient approximation made simple. Physical Review Letters. 77, 3865.
4. Kresse, G., Joubert, D. (1999). From ultrasoft pseudopotentials to the projector augmented-wave method. Physical Review B. 59, 1758.
5. Kresse, G., Furthmüller, J. (1996). Efficiency of ab-initio total energy calculations for metals and semiconductors using a plane-wave basis set. Computational Materials Science. 6, 15–50.
6. Kresse, G., Furthmüller, J. (1996). Efficient iterative schemes for ab initio total-energy calculations using a plane-wave basis set. Physical Review B. 54, 11169.
7. Heyd, J., Scuseria, G.E., Ernzerhof, M. (2003). Hybrid functionals based on a screened Coulomb potential. The Journal of Chemical Physics. 118, 8207–8215.